

High-temperature cuprate superconductors studied by x-ray Compton scattering and positron annihilation spectroscopies

Bernardo Barbiellini

Department of Physics, Northeastern University, Boston MA 02115, USA

The bulk Fermi surface in an overdoped ($x = 0.3$) single crystal of $\text{La}_{2-x}\text{Sr}_x\text{CuO}_4$ has been observed by using x-ray Compton scattering. This momentum density technique also provides a powerful tool for directly seeing what the dopant Sr atoms are doing to the electronic structure of La_2CuO_4 . Because of wave function effects, positron annihilation spectroscopy does not yield a strong signature of the Fermi surface in extended momentum space, but it can be used to explore the role of oxygen defects in the reservoir layers for promoting high temperature superconductivity.

PACS numbers: 74.72.-h, 78.70.Ck, 78.70.Bj, 71.10.Ay

I. INTRODUCTION

Discovered by Bednorz and Müller in 1986 [1], high temperature superconductivity in cuprates has mobilized scientists around the world, both to understand its origin and to find new compounds with higher superconducting transition temperature T_c .

The lanthanum compounds $\text{La}_{2-x}\text{M}_x\text{CuO}_4$ have variable impurity content x and $\text{M} = \text{Ca}, \text{Ba}, \text{Sr}$. Their crystal structure, shown in Fig. 1, belongs to the K_2NiF_4 family. It is built up from Cu-O superconducting layers alternating with rock salt type layers, which provide the charge reservoirs. When $x = 0$, these materials have antiferromagnetic insulating phases. It is only with increasing x that the metallic state and superconductivity set in. A naive chemical argument finds that, when $x = 0$, copper has a valency +2 and thus contains one hole (missing electron). The increase of x creates excess of holes that causes the oxides to conduct.

However, the physics and chemistry of doping high-temperature cuprate superconductors still remain something of a mystery. For instance, standard theories cannot readily explain the sudden destruction of superconductivity at high doping concentrations. For this reason, we have undertaken [2] Density Functional Theory (DFT) calculations for nano-sized supercells of La_2CuO_4 with dopants. These calculations show that weak ferromagnetism appears around clusters of high Ba concentration and suggest that ferromagnetism and superconductivity compete in overdoped samples. Our studies on doping have also shown how by scattering high energy x-rays from single crystals of $\text{La}_{2-x}\text{Sr}_x\text{CuO}_4$, one can directly image the character of holes doped into this material [3]. At low doping the hole O $2p$ character is much stronger than the Cu $3d$ character. However, at high doping the Cu $3d$ character becomes dominant. These observations are highly significant because via x-ray scattering we have new tools for directly seeing what the dopant atoms are doing in these materials [4]. The same advanced x-ray characterization could be used to study cathode materials for lithium batteries [5], where the octahedron formed by a transition metal atom and six oxygen atoms plays a key role like the CuO_6 building

block in the La_2CuO_4 compound (see Fig. 1).

Since high T_c superconductivity appears to be near a metal-insulator transition there is a particular significance attached to the existence of the Fermi Surface (FS) in the normal state. Currently, the only direct probe of FS is angle-resolved photoemission (ARPES) [6]. While ARPES has many strengths, this has created the problem that most of our understanding of cuprates is based on measurements from a single, surface sensitive technique that has been applied only to a limited number of materials that cleave. Thus, the risk is that experimental artifacts can be interpreted as fundamental physics. Therefore, it is important to develop new approaches to measuring both electron momentum density and FS applicable to a much wider class of materials.

II. 2D ACAR SPECTROSCOPY

The two dimensional angular correlation of positron annihilation radiation (2D ACAR) [7–9] depends, by momentum and energy conservation, on the two photon momentum density $R(p)$ of an annihilating electron-positron pair [10, 11]. Given a typical electronic momentum $|p| \sim 10^{-2}mc$, the angle between the two photons deviates only by a few milliradians from anticollinearity, since each photon has momentum $\sim mc$ (energy $\sim mc^2$). Thus angles θ_x and θ_y are directly related to the $p_x = mc\theta_x$ and $p_y = mc\theta_y$ components of p . The two dimensional (2D) ACAR spectrum is measured by γ detectors at a large distance from the sample (about 10 meters). Then one obtains the projection of $R(\mathbf{p})$

$$N(p_x, p_y) = \int dp_z R(\mathbf{p}). \quad (1)$$

Actually, the distribution $N(p_x, p_y)$ is convoluted with the resolution function of the experimental setup and the typical experimental resolution is of the order 0.03 a.u. of momentum. The 2D ACAR has been successful for a determination of the FS in many metallic systems [11], but similar studies of the high- T_c oxides have met difficulties [4, 9]. Although the electron-positron momentum density measured in a positron-annihilation experiment contains

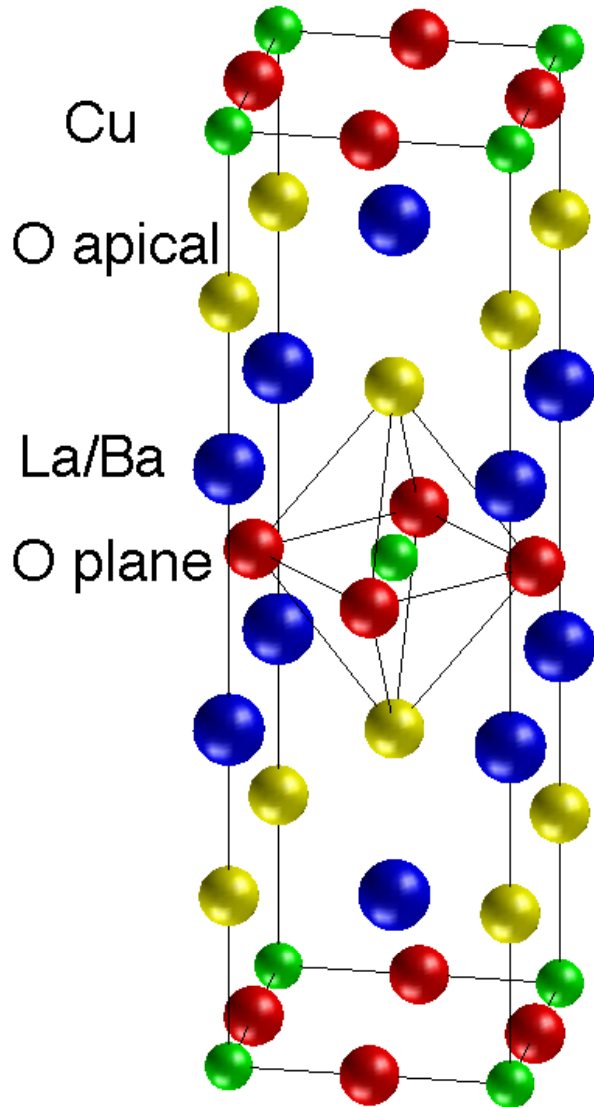


FIG. 1: The structure of $\text{La}_{2-x}\text{Ba}_x\text{CuO}_4$. The La and Ba atoms (blue spheres) are in the charge reservoir layers, which contains all the dopant atoms. The so-called apical O atoms (yellow spheres) are located in the same layers while the Cu atoms (green spheres) and the planar O atoms (red spheres) belong to the superconducting layers. The CuO_6 octahedron (shown in the middle) is formed by a CuO_4 plaquette and two apical O atoms and determines the important $x^2 - y^2$ and z^2 features of the electronic structures.

FS signatures, the amplitude of such signatures is controlled by the extent to which the positron wave function overlaps with the states at the Fermi energy. Calculations of the positron density distribution indicates that the positron does not probe well the FS contribution of the Cu-O planes in $\text{La}_{2-x}\text{Sr}_x\text{CuO}_4$ [12]. Indeed, we see little evidence of FS signatures in either the computed or

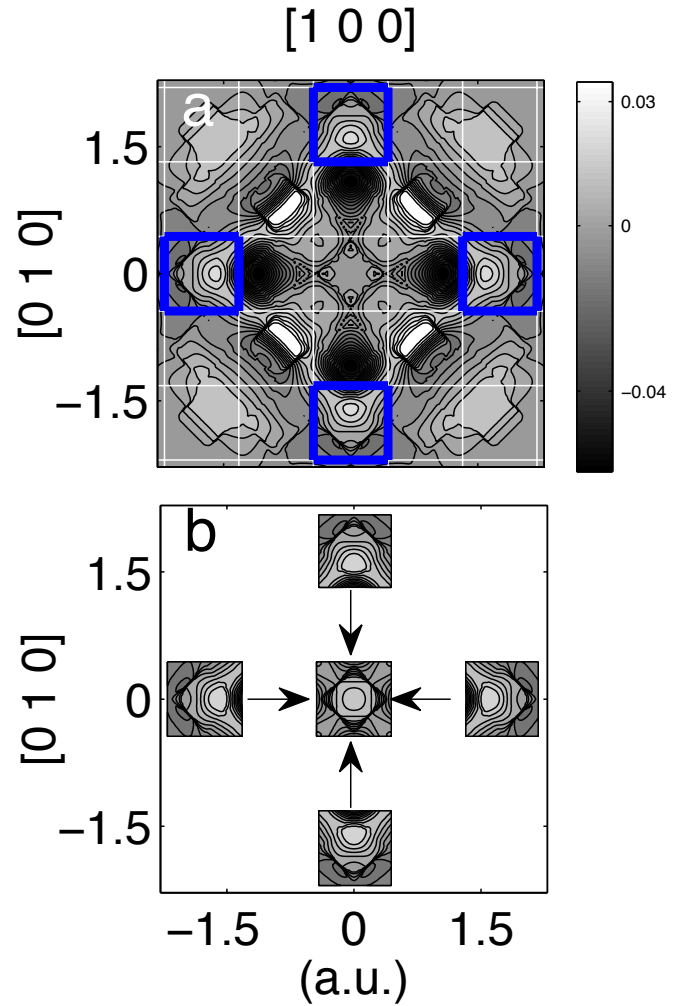


FIG. 2: FS analysis from the 2D electron momentum density distribution: a) Cylindrical anisotropy for theoretical electron momentum density. The white lines define the Brillouin zones, while blue squares indicate a family of zones where the FS features are particularly strong. (b) The blue squared regions are isolated from the rest of the spectra and folded back to the central region. The color scale is in units of the 2D momentum density at the origin. The total amplitude of the 2D momentum density anisotropy is of the order of 8% in excellent agreement with the experiment.

the measured 2D ACAR distributions.

III. X-RAY COMPTON SCATTERING SPECTROSCOPY

Compton scattering refers to inelastic x-ray scattering [13–15] in the deeply inelastic limit in which the non-resonant scattering cross-section is well-known to become

proportional to the ground state momentum density [16]. Compton scattering thus provides a uniquely powerful probe of the many body ground state wave function. The technique is also well suited for investigating disordered alloys because, being a ground state probe, it does not require long electron mean free paths. By contrast, transport type experiments such as the De Haas-van Alphen effect are limited to low defect and impurity concentrations. Like other light scattering techniques, Compton scattering is genuinely a bulk probe, which is not complicated by the presence of surface effects involved in ARPES. Historically, the capabilities of the Compton technique have been slow to realize in practice because only a limited momentum resolution (~ 0.4 a.u.) was possible with gamma ray sources. However, with the availability of second and third generation synchrotron light sources and improvements in detector technology, it has become possible now to achieve momentum resolution of about 0.1 a.u. in wide classes of materials, and of about 0.01 a.u. in low-Z systems [13, 17]. These advances have sparked a renewed interest in Compton scattering as a tool for investigating Fermi liquid and bonding related issues and also as a unique window on hitherto inaccessible correlation effects in the electron gas. We have developed extensive methodology for obtaining momentum density and highly accurate Compton profiles (CPs) within the Fermi liquid framework [11, 18] and generalized it to the correlated Resonating valence bond (RVB) ground state [19, 20]. These studies have shown, for example, the surprising degree to which Li deviates from the Fermi liquid paradigm [21]. These results have also prompted us to look for ways of going beyond the standard DFT framework by using antisymmetric geminal products (AGP) of pair wavefunctions to construct the many-body state in a solid. The AGP is an important building block of the RVB. This scheme can be applied to highly correlated electron systems such as high temperature superconductors. In the ground state of these materials, multi-configuration effects lead to non-integer occupancies of one-electron states. The AGP and RVB calculations have shown that the deviation from integer occupancy becomes stronger as correlations grow. However, the important finding of our recent work in an overdoped ($x = 0.3$) single crystal of $\text{La}_{2-x}\text{Sr}_x\text{CuO}_4$ [12] is that strong correlation effects that ordinarily reduce the Compton anisotropy amplitudes are no longer effective at this doping. The quantitative agreement between DFT calculations and momentum density experiments (2D ACAR and 2D Compton scattering reconstruction) shown in Ref. [12] suggests that Fermi liquid physics is restored in the overdoped regime. A FS signal was also clearly observed by Compton scattering in the third Brillouin zone along [100] and the calculated FS topology was found to be in good accord with the corresponding experimental data. In particular, Fig 2 (a) shows the cylindrical anisotropy of the theoretical 2D electron moment density. Because the FS is periodic, a complete FS must exist in each Brillouin zone, but with its intensity modu-

lated by electronic wave functions effects. For a predominantly d character at the FS, these wave functions will strongly suppress spectral weight near the origin, so the FS breaks are most clearly seen in higher Brillouin zones. These FS breaks appear superimposed on the momentum density in the form of discontinuities which can occur in any Brillouin zone. In Fig.2 (a), the Fermi surface breaks are the regions where the contours run closely together. This means that the electron momentum density varies rapidly at these locations. Fig.2 (a) shows the calculated Fermi breaks in several Brillouin zones. In particular, in the third zones framed with blue squares, the arc-like features are theoretically predicted FSs associated with Cu-O planes. Due to the tetragonal symmetry, a rotation of the spectrum by $\pi/2$ will generate symmetry-related regions (blue squares) with equivalent strong FS features. These regions are isolated in Fig.2 (b). By folding back only these regions as shown by the arrows of Fig.2 (b), we produce a full FS, where strong wave functions effects are substantially circumvented.

IV. OXYGEN DEFECTS IN HIGH TEMPERATURE SUPERCONDUCTORS

The positron lifetime is an ideal tool to detect low concentrations of defects in materials [10]. It is determined by the positron-electron contact density, which is remarkably higher than the unperturbed electron density [9]. The ratio of these two densities is called the *enhancement factor* and it is used in ACAR calculations as well. The agreement between the positron annihilation theory and the experiment is usually excellent within the Generalized Gradient Approximation (GGA) [22, 23]. The GGA can also be safely applied for the calculation of positron annihilation rates at defects in cuprates [24].

Curiously, it has been difficult to obtain cuprates single crystals of a sufficient size and perfection. In fact, some of these substances have atomic defects such as oxygen vacancies and interstitials, others contain charge density waves and some others present themselves with a number of different phases. Are all these only accidental complications of minor importance to high temperature superconductivity? Or, are they on the contrary connected to essential properties of high temperature superconductivity? An empirical law [25] (only valid for high temperature superconductors) suggests that

$$k_B T_c \tau \sim \hbar, \quad (2)$$

where k_B is the Boltzmann's constant, \hbar is the Planck constant, T_c is the superconducting critical temperature and τ is the electron relaxation time in the normal state. Therefore, in order to increase T_c , one can increase the electron scattering (i.e. lower τ) by introducing certain impurities or defects. The intense level of scattering given by Eq. 2 corresponds to the so-called *Planckian dissipation limit*, beyond which Bloch-wave propagation becomes inhibited, i.e. the quasi-particle states themselves

become incoherent. The fact that the relaxation rate $1/\tau$ scales with T_c implies that the interaction causing this anomalous scattering is also associated with the superconducting pairing mechanism [26].

Interestingly, a different route to hole doping is to introduce excess of oxygen in the La_2CuO_4 compound, which is possible because there are extra sites in the reservoir layers for the oxygen atoms to occupy. $\text{La}_2\text{CuO}_{4+\delta}$ when doped in the range of $0.1 \leq \delta \leq 0.12$ achieves the best T_c , however the form of the oxygen interstitials distribution [27] can change both T_c and τ dramatically. So far as the technique of positron spectroscopy is concerned, it has become clear that the propensity to oxygen defects [24] has an essential influence on positron annihilation measurements. For example, we have shown that positrons are trapped at oxygen vacancies in the superconducting compound $\text{YBa}_2\text{Cu}_3\text{O}_{7-\delta}$ while this trapping becomes negligible in the non-superconducting sample where Y has been replaced by Pr [28]. Our goal is therefore to show via positron annihilation spectroscopy that oxygen defects (both interstitials and vacancies) are connected to essential properties of high temperature superconductivity [29].

V. CONCLUSION

The quantitative agreement between the calculations and the experiment for ACAR as well as momentum

density anisotropies suggests that $x = 0.3$ overdoped $\text{La}_{2-x}\text{Sr}_x\text{CuO}_4$ can be explained within the conventional Fermi-liquid theory. The FS analysis from Compton scattering confirms previous ARPES FS measurements showing an electron-like FS in the overdoped regime. This validation is important since we provide via deep inelastic x-ray scattering experiments a truly bulk-sensitive image of momentum density maps of electrons near the Fermi level. In general, this momentum density information is difficult to extract from ARPES experiments due to difficulties associated with matrix element effects and the well-known surface sensitivity of ARPES. However, improvements in the momentum resolution are still needed to bring Compton scattering into the fold of mainstream probes for the cuprates FS. Higher momentum resolution can also enable the study of the FS smearing due to the superconducting energy gap opening [9]. Positron annihilation spectroscopy cannot probe well the FS of the Cu-O layers, but it can be extremely useful to explain why oxygen defects at reservoir layers play an important role in high temperature superconductivity [29].

Acknowledgments: This work is supported by the US-DOE, Grants No. DE-FG02-07ER46352 and No. DE-FG02-08ER46540 (CMSN) and benefited from the allocation of supercomputer time at NERSC and Northeastern University Advanced Scientific Computation Center (ASCC).

-
- [1] J.C. Bednorz and K.A. Müller, *Z. Phys. B* **64** (1986) 180
 [2] B. Barbiellini and T. Jarlborg, *Phys. Rev. Lett.* **101** (2008) 157002
 [3] Y. Sakurai, M. Itou, B. Barbiellini, P. E. Mijnders, R. S. Markiewicz, S. Kaprzyk, J.-M. Gillet, S. Wakimoto, M. Fujita, S. Basak, Yung Jui Wang, W. Al-Sawai, H. Lin, A. Bansil, and K. Yamada, *Science* **332** (2011) 698
 [4] B. Barbiellini and P.M. Platzman, *Mat. Sci. Forum* **255-257** (1997) 189
 [5] Xiaosong Liu, Jun Liu, Ruimin Qiao, Yan Yu, Hong Li, Liumin Suo, Yong-sheng Hu, Yi-De Chuang, Guojun Shu, Fangcheng Chou, Tsu-Chien Weng, Dennis Nordlund, Dimosthenis Sokaras, Yung Jui Wang, Hsin Lin, Bernardo Barbiellini, Arun Bansil, Xiangyun Song, Zhi Liu, Shishen Yan, Gao Liu, Shan Qiao, Thomas J. Richardson, David Prendergast, Zahid Hussain, Frank M. F. de Groot and Wanli Yang, *J. Am. Chem. Soc.* **134** (2012) 13708
 [6] A. Damascelli, Z. Hussain, Z.-X. Shen, *Rev. Mod. Phys.* **75** (2003) 473
 [7] S. Berko, M. Hagooie and J.J. Mader, *Phys. Lett. A* **63** (1977) 335
 [8] P.E. Bisson, P. Descouts, A. Dupanloup, A.A. Manuel, E. Perreard, M. Peter and R. Sachot, *Helv. Phys. Acta* **55** (1982) 110
 [9] M. Peter, T. Jarlborg, A.A. Manuel, B. Barbiellini, S.E. Barnes, *Z. Naturforsch.* **48a** (1993) 390
 [10] B. Barbiellini, in *New Directions in Antimatter Chemistry and Physics*, edited by C. M. Surko and F. A. Gianturco (Kluwer Academic Publishers, The Netherlands, 2001)
 [11] B. Barbiellini, S. B. Dugdale and T. Jarlborg, *Computational Materials Science* **28** (2003) 287
 [12] W. Al-Sawai, B. Barbiellini, Y. Sakurai, M. Itou, P. E. Mijnders, R. S. Markiewicz, S. Kaprzyk, S. Wakimoto, M. Fujita, S. Basak, H. Lin, Yung Jui Wang, S. W. H. Eijt, H. Schut, K. Yamada, and A. Bansil, *Phys. Rev. B* **85** (2012) 115109
 [13] E.D. Isaacs, P.M. Platzman, *Physics Today* (February 1996) 40
 [14] Yung Jui Wang, B. Barbiellini, Hsin Lin, Tanmoy Das, Susmita Basak, P. E. Mijnders, S. Kaprzyk, R. S. Markiewicz, and A. Bansil, *Phys. Rev. B* **85** (2012) 224529
 [15] B. Barbiellini, P. Nicolini, *Phys. Rev. A* **84** (2011) 022509
 [16] I. G. Kaplan, B. Barbiellini, A. Bansil, *Phys. Rev. B* **68** (2003) 235104
 [17] M. J. Cooper, P. E. Mijnders, N. Shiotani, N. Sakai, and A. Bansil, *X-Ray Compton Scattering* (Oxford University Press, Oxford, 2004)
 [18] A. Bansil, B. Barbiellini, S. Kaprzyk and P.E. Mijnders, *J. Phys. Chem. Solids* **62** (2001) 2191
 [19] B. Barbiellini, *J. Phys. Chem. Solids* **61** (2000) 341
 [20] B. Barbiellini, A. Bansil, *J. Phys. Chem. Solids* **62** (2001) 2181
 [21] D. Nissenbaum, L. Spanu, C. Attacalite, B. Barbiellini

- and A. Bansil, Phys. Rev. B **79** (2009) 03541
- [22] B. Barbiellini, M. J. Puska, T. Torsti and R. M. Nieminen, Phys. Rev. B **51** (1995) 7341
- [23] B. Barbiellini, M. J. Puska, T. Korhonen, A. Harju, T. Torsti and R. M. Nieminen, Phys. Rev. B **53** (1996) 16201
- [24] B. Barbiellini, M. J. Puska, A. Harju and R. M. Nieminen, J. Phys. and Chem. of Solids **56** (1995) 1693
- [25] J. Zaanen, Nature **430** (2004) 512
- [26] N. E. Hussey, R. A. Cooper, Xiaofeng Xu, Y. Wang, I. Mouzopoulou, B. Vignolle and C. Proust, Phil. Trans. R. Soc. A **369** (2011) 369
- [27] M. Fratini, N. Poccia, A. Ricci, G. Campi, M. Burghammer, G. Aeppli and A. Bianconi, Nature **466** (2010) 841
- [28] A. Shukla, L. Hoffmann, A.A. Manuel, E. Walker, B. Barbiellini and M. Peter, Phys. Rev. B **51** (1995) 6028
- [29] T. Jarlborg, B. Barbiellini, R.S. Markiewicz and A. Bansil, Phys. Rev. B **86** (2012) 235111